Theoretical Prediction of Isotope Effects on Charge Transport in Organic Semiconductors

Yuqian Jiang,[†] Hua Geng,[‡] Wen Shi,[†] Qian Peng,[‡] Xiaoyan Zheng,[†] and Zhigang Shuai*,[†]

[†]MOE Key Laboratory of Organic OptoElectronics and Molecular Engineering, Department of Chemistry, Tsinghua University, Beijing 100084, People's Republic of China

[‡]Key Laboratory of Organic Solids, Beijing National Laboratory for Molecular Sciences (BNLMS), Institute of Chemistry, Chinese Academy of Sciences, Beijing 100190, People's Republic of China

ⓢ *Supporting Information*

ABSTRACT: We suggest that the nuclear tunneling effect is important in organic semiconductors, which we showed is absent in both the widely employed Marcus theory and the band-like transport as described by the deformation potential theory. Because the quantum nuclear tunneling tends to favor electron transfer while heavier nuclei decrease the quantum effect, there should occur an isotope effect for carrier mobility. For *N,N'-n*-bis(*n*-hexyl)-naphthalene diimide, electron mobility of all-deuteration on alkyls and all ^{13}C-substitution on the backbone decrease ~18 and 7%, respectively. Similar isotope effects are found in the *N,N'-n*-bis(*n*-octyl)-perylene diimide. However, there is nearly no isotope effect for all-deuterated rubrene or tetracene. We have found that the isotopic effect only occurs when the substituted nuclei contribute actively to vibrations with appreciable charge reorganization energy and coupling with carrier motion. Thus, this prediction can shed light on the current dispute over the hopping versus band-like mechanisms in organic semiconductors.

$$k^{QM} = \frac{|V|^2}{\hbar^2} \int_{-\infty}^{\infty} dt \quad \text{Nuclear Tunneling Model}$$
$$\exp\left\{-\sum_j S_j\left[(2\bar{n}_j+1)-\bar{n}_j e^{-i\omega_j t}-(\bar{n}_j+1)e^{i\omega_j t}\right]\right\}$$

−20% −18% −7% −1%

Isotope Effect: The Reduction of Mobility

SECTION: Energy Conversion and Storage; Energy and Charge Transport
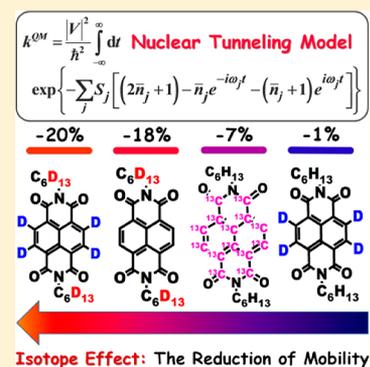
In recent years, charge transports have been extensively studied for organic semiconductors.[1−3] However, there is still controversy over the mechanism, being hopping or band-like. Experimentally, the temperature dependence of mobility is generally a standard to judge the transport mechanism. When mobility increases with the rising temperature, thermally activated hopping transport is considered to be dominant, where the charge reorganization energy (λ) is much larger than the intermolecular electron coupling (V), and the charge is considered to be fully localized on a single molecule. Semiclassical (SC) Marcus theory has been widely used to study the hopping behavior combined with quantum chemistry calculations as advocated by Brédas and co-workers.[4−6] Such a description has been applied from evaluating molecular parameters for materials design to obtaining more quantitative determination of charge mobility with success.[7−9] The adiabatic transition described by Marcus theory is assumed to be a thermally activated process of which the mobility is expected to vanish when the temperature goes to 0 K. On the other hand, when the mobility decreases with temperature, the band-like model is proposed, and the existence of small polaron has been questioned.[10,11] An alternative mechanism such as dynamic disorder-limited transport has also been proposed[12,13] to explain such a temperature dependence of mobility, which is essentially a band-like picture but with temperature-dependent off-diagonal disorder. However, several recent experimental results demonstrate that the temperature dependence of mobility is not enough for clarifying the transport mechanism.

For example, in situ charge modulation spectroscopy on organic field effect transistor with 6,13-bis-(triisopropylsilylethynyl) (TIPS)-pentacene as the active layer indicates that the transporting carriers come from localized charges, even at very low temperature, while the mobility decreases with temperature, behaving "paradoxically" band-like.[14,15] The temperature-independent transport has been found in high-mobility dinaphtho-thieno-thiophene (DNTT) single crystal transistors, which was claimed to be as band-like transport.[1] Therefore, more investigations are needed to understand the charge-transport mechanism in organic systems.

The "exotic" behavior in TIPS-pentacene has been studied by our previously proposed quantum nuclear tunneling model for the localized charge transfer (CT) formalism in organic semiconductors.[16] When coupled with quantum chemistry calculation, both qualitative and quantitative agreements with experiment have been achieved for TIPS-pentacene.[17] The nuclear tunneling effect is found to lower the activated energy barrier for carrier hopping because of the high-frequency modes from conjugated carbon−carbon stretching vibrations,[16] so that "band-like" mobility can be predicted from the hopping model. The full quantum CT rate formula[16,18] reads

$$k^{QM} = \frac{|V|^2}{\hbar^2} \int_{-\infty}^{\infty} dt \, \exp\left\{-\sum_j S_j[(2\overline{n}_j + 1) - \overline{n}_j e^{-i\omega_j t} - (\overline{n}_j + 1)e^{i\omega_j t}]\right\} \tag{1}$$

where V is the intermolecular transfer integral as shown in Figure 1. $\overline{n}_j = 1/[\exp(\hbar\omega_j/k_B T) - 1]$ is the occupation number
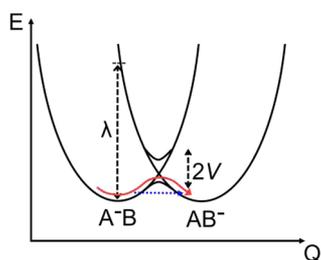
Figure 1. Schematic representation of electron transfer from molecule A to molecule B in a quantum well. The SC Marcus hopping pathway is labeled as a solid red arrow, while the nuclear tunneling mechanism is labeled with a dashed blue arrow.

for the jth vibrational mode with frequency ω_j, and S_j is the Huang–Rhys factor relating to the jth mode, which represents the local electron–phonon coupling. In the limit of strong coupling ($\sum_j S_j \gg 1$) with short-time approximation ($\exp(i\omega t) = 1 + i\omega t + (i\omega t)^2/2$) and at high temperature ($\hbar\omega_j/k_B T \ll 1, \overline{n}_j \approx k_B T/\hbar\omega_j$), eq 1 goes back to the SC Marcus formula

$$k^{SC} = \frac{|V|^2}{\hbar}\left(\frac{\pi}{\lambda k_B T}\right)^{1/2} \exp\left(-\frac{\lambda}{4k_B T}\right) \tag{2}$$

where the reorganization energy is $\lambda = \sum_j \lambda_j = \sum_j S_j \hbar\omega_j$, as shown in Figure 1.

Interestingly, such a quantum nuclear tunneling picture was adopted recently to elucidate a recent dispute over the transport mechanism in conducting polymers. Three mutually exclusive models had been proposed to explain the conductivity power law of $J(V,T)$, the one-dimensional Luttinger liquid model,[19] the environment Coulomb blockade model,[20] and the modified variable range hopping.[21] On the basis of the quantum nuclear tunneling picture under an external field, Asadi et al. derived a macroscopic current expression that was found to be universal for various polymers at all temperatures and voltages.[22] In addition, finite conductivity in polymers has been observed at low temperatures in several experiments.[23,24] This picture has been further elucidated theoretically from a time-dependent wavepacket dynamics (TDWPD); the nuclear tunneling caused by high-frequency intramolecular vibrations with large local electron–phonon coupling could be fast enough to break down the electronic coherence between two adjacent sites, justifying the hopping model with a quantum nuclear tunneling effect.[25−27] All of these point to the importance of the long-ignored nuclear tunneling effect in organic and polymeric semiconductors, even though the nuclear tunneling effect for a small polaron[28,29] had been proposed long ago. However, there has been no direct experimental verification for the nuclear tunneling effect in organic semiconductors.

In this work, we propose a theoretical prediction on isotope effects to further manifest the nuclear tunneling effect, which is expected to help to reveal the charge-transport mechanism, namely, the isotope effect is naturally expected if nuclear-

tunneling-assisted hopping is the mechanism, but it is absent in other mechanisms. According to Marcus theory in eq 2, there would be no isotope effect because both V and λ are independent of isotope substitution. On another hand, for the band-like transport, where often the electron coherent length reaches a few nanometers like in single-crystal silicon, much longer than the lattice spacing, the acoustic phonon scattering becomes the major source of carrier scattering. Then, according to Boltzmann transport theory and the deformation potential theory,[30,31] there should be no isotope effect either because the acoustic-deformation-caused energy level shift is independent of the isotope (see the Supporting Information (SI)). Only when the quantum nature of nuclear motion is considered, where heavier atoms can weaken the quantum effect while keeping the same electronic structure, the charge mobility is expected to be reduced and approach the SC end. Hence, the isotope effect would be a direct manifestation of quantum nuclear tunneling in the hopping model. Therefore, the isotope effect can only be manifested in the case of nuclear tunneling in a hopping picture or in the case of optical phonon scattering in a band-like picture, which is ignored in the deformation potential theory. Thus, investigating the isotope effect in transport can indeed shed light on revealing the carrier transport mechanism.

There are very few experiments on the isotope effect for charge transport so far. A recent experimental investigation on hole mobility for all-deuterated rubrene ($C_{42}D_{28}$) indicates that there is no noticeable isotope effect for $C_{42}D_{28}$.[32] Nevertheless, the isotope effect has been widely investigated in understanding the mechanism of chemical reactions[33−35] and excited-state nonradiative decay processes.[36−38] In chemical reaction dynamics, isotopic substitution can drastically modify the rate when the replacement occurs in a chemical bond that is broken or formed. Deuteration on some light-emitting organic molecules can influence the $T_1 \rightarrow S_0$ or $S_1 \rightarrow S_0$ nonradiative decay rate. These can be rationalized by mass affecting the vibrational frequency of the chemical bonds or phonon modes, while the electron configurations are identical.

We take n-type materials N,N'-bis(n-hexyl)-naphthalene diimide (NDI-C6) and N,N'-bis(n-octyl)-perylene diimide (PDI-C8) as examples,[39−42] for which $\lambda \gg V$, to study their isotope effect by our quantum nuclear tunneling model. Changing a hydrogen atom (H) to deuterium (D) represents a 100% increase in mass, which is the greatest among all isotopic substitutions, whereas replacing ^{12}C with ^{13}C, the mass increases by only 8%, which is much less than deuteration. However, in organic materials, the stretching vibrations of the carbon backbone are the major scattering modes for the carrier. Therefore, we investigate both deuterium and ^{13}C isotopic effects on charge transport. Four different isotopic substitutions for both NDI-C6 and PDI-C8 are here considered, namely, all-deuterated (**N1, P1**), alkyl chain only deuterated (**N2, P2**), backbone-deuterated (**N3, P3**), and all-backbone ^{13}C-substituted (**N4, P4**), along with the pristine NDI-C6 (**N0**) and PDI-C8 (**P0**) (see Figure 2). In addition, for NDI-C6, backbone carbon partly substituted by ^{13}C (**N5**) is also considered.

The intermolecular transfer integral V in eq 1 or 2 can be calculated by numerous methods, for example, the energy level splitting method,[5] the minimized energy level splitting along the reaction path method,[43] the direct evaluation method,[44,45] and the site-energy-corrected coupling method.[46] According to the benchmark study of their performances,[47] the last three

(a)

N1: all H→D　　　　　　　　N4: all ^{12}C→^{13}C in backbone

N2: all H→D in n-C_6H_{13}　　　N5: 4 selected ^{12}C→^{13}C in backbone (labeled 1~4)

N3: all H→D in backbone

(b)

P1: all H→D　　　　　　　　P3: all H→D in backbone

P2: all H→D in n-C_8H_{17}　　P4: all ^{12}C→^{13}C in backbone

Figure 2. Schematic presentation of isotopically substituted (a) NDI-C6 and (b) PDI-C8.

Table 1. Room-Temperature Electron Mobility (μ_e, cm^2/(V s)) Calculated by the Nuclear Tunneling Model and the Corresponding Isotope Effect (IE, %) on Mobility Defined as $(\mu_{Ni} - \mu_{N0})/\mu_{N0}$ for All Isotopically Substituted Systems^a

NDI-C6	μ_e	IE	PDI-C8	μ_e	IE
N0	4.31	0.00	P0	13.19	0.00
N1	3.44	−20.18	P1	11.11	−15.77
N2	3.55	−17.63	P2	11.53	−12.58
N3	4.27	−0.93	P3	12.89	−2.27
N4	4.02	−6.73	P4	11.87	−10.01
N5	4.28	−0.70			
Marcus	0.24		Marcus	0.50	
exp.	0.7^b		exp.	1.7^c	

^{a}The electron mobility calculated from Marcus theory and the experimental data of pristine systems are also given for comparison. ^{b}Reference 40. ^{c}Reference 42.

a remarkable isotope effect in both NDI-C6 and PDI-C8. Namely, the mobility is reduced upon isotope substitution. Especially for the all-deuterated NDI-C6 and PDI-C8, the decreases in charge mobility reach 20 and 16%, respectively. In contrast, there is no noticeable isotope effect for the backbone-deuterated systems (N3, P3) as well as four ^{13}C-substituted NDI-C6 (N5). Even though the mobility obtained from the quantum CT method is about an order of magnitude higher than the experimental results, it should be noted that the experimental mobility depends on several external factors, including the device fabrication condition, material processes, disorder, and impurities. Furthermore, the electron mobility of NDI and PDI derivatives such as dichloro-substituted NDI[3] and dicyano-substituted PDI[49] can reach up to 6−8 cm^2/(V s) nowadays. The theoretical calculations cannot only reveal the underlying transport mechanism but also serve as the intrinsic value.

For comparison, the Marcus formula for all six compounds of NDI-C6 gives completely the same result, $k^{SC} = 5.20 \times 10^{12}$ s^{-1} for a dimer with the largest intermolecular transfer integral and electron mobility $\mu_e = 0.24$ cm^2/(V s). For PDI-C8, the five substitutions present the same electron mobility 0.50 cm^2/(V s). Quantum chemistry calculation confirms that there is no isotope effect in the SC theory. It is also noted that Marcus theory even underestimates the mobility; the theoretical value is usually considered as an upper limit because there are more scattering sources in materials such as impurities or disorders.

We thus predict that the all-deuterated NDI-C6 and PDI-C8 can reduce the room-temperature electron mobility by ∼20 and ∼16%, and all ^{13}C-substitution on backbones of NDI-C6 and PDI-C8 can reduce mobility by ∼7 and ∼10%, respectively. The isotope effect obtained by the nuclear tunneling model can be rationalized by analyzing the vibronic coupling. According to eq 1, the CT rate depends on S_j, ω_j, and their populations; isotopic substitution does not modify V. The total reorganization energy can be projected into vibrational relaxation. Modes with large S_j indicate strong scattering with the charge carrier. When such modes are affected by isotope substitution, the frequencies decrease, and the tunneling ability is weakened accordingly. Because the total reorganization energy is unchanged, lowering frequencies implies increasing coupling strength, thus reducing the CT rate, or mobility.

To better understand how different isotopic substitutions affect the charge transport, we take NDI-C6 as an example for normal-mode analysis. We depict the five vibrational modes

methods give similar results. Here, V between molecules m and n is calculated with the site-energy-corrected coupling method, which can be expressed as $V_{mn} = [V^0_{mn} - (1/2)(e_m + e_n)O_{mn}]/[1 - O^2_{mn}]$, where $e_m = \langle \phi_m|H|\phi_m \rangle$, $V^0_{mn} = \langle \phi_m|H|\phi_n \rangle$, and $O_{mn} = \langle \phi_m|O|\phi_n \rangle$. $\phi_{m(n)}$ is the frontier molecular orbital of an isolated molecule m(n) in the dimer. For hole (electron) transport, the HOMO (LUMO) should be plugged in. H and O are the dimer Hamiltonian and the overlap matrices, respectively. By combining quantum chemistry calculation and normal-mode analysis, the quantum CT rate expressed in eq 1 can be obtained. The charge mobility can be obtained through the Einstein formula $\mu = eD/k_BT$ by assuming a diffusion process. The diffusion constant D is simulated via a kinetic Monte Carlo simulation. The charge hops between nearest-neighboring molecules with a probability $p_\alpha = k^\alpha_{mn}/\sum_\alpha k^\alpha_{mn}$ for the αth pathway, and the simulation time is incremented by $1/\sum_\alpha k^\alpha_{mn}$.[48] The 3D diffusion coefficient is obtained as $D = \langle l^2 \rangle/6t$ averaged over 8000 trajectories. We repeat it 100 times, and the average mobility is evaluated as $(1/100)\sum_i^{100} \mu_i$.

The electron mobility for all NDI-C6 and PDI-C8 compounds is calculated and presented in Table 1. It is seen that the all-deuterated (N1, P1), alkyl-chain-deuterated (N2, P2), and all-backbone ^{13}C-substituted (N4, P4) systems exhibit

with the most significant contributions to the charge reorganization in Figure 3, and their corresponding frequencies
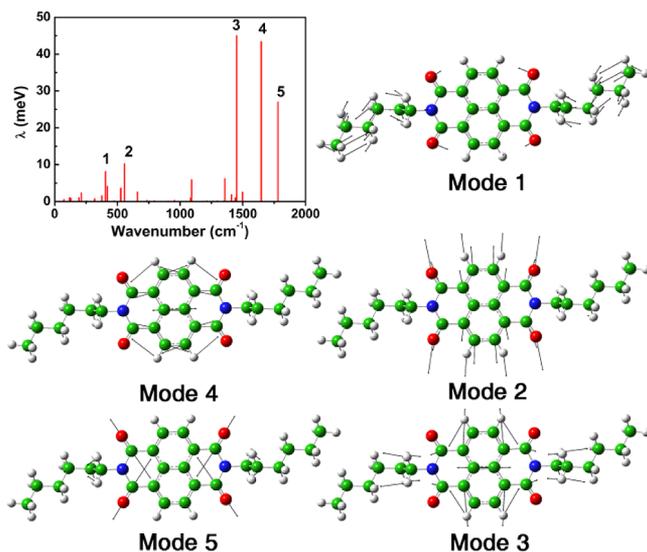
Figure 3. Reorganization energy distribution of pristine neutral NDI-C6 and five vibrational modes with the most significant contributions to the reorganization energy.

for each isotopic substitution are listed in Table 2. More data are given in Tables S6 and S9 in SI. From Table 2, we find that the frequencies of mode 1 for **N1** and **N2** and the frequencies of modes 2−5 for **N4** are reduced remarkably after isotopic substitution, while all five modes for **N3** and **N5** undergo small reduction upon isotope substitutions. From Figure 3, we can see that mode 1 mainly includes rocking vibrations of n-C$_6$H$_{13}$, so that the large mass increase caused by all-deuteration on alkyls in **N1** and **N2** can reduce the frequency effectively. Mode 2 is the in-plane bending of the aromatic ring, modes 3 and 4 are mainly conjugated C−C stretching vibration in the backbone, and mode 5 is mainly C=O stretching vibration; thus, all ^{13}C-subsition on backbone can lead to a significant decrease in the frequencies of modes 2−5. For PDI-C8 systems, the situation is similar to NDI-C6 because the vibrational modes and the reorganization energy distribution are very similar (see SI Tables S7 and S10).

However, it is noted that the recent experiment for all-deuterated rubrene did not show any appreciable isotope

effect.[32] We thus extend our approach to rubrene. Note that it was proposed that rubrene might be best described by a band-like model.[11] Nevertheless, one recent experiment showed that the transport in tetracene was indeed governed by the hopping mechanism,[50] implying the adequacy of our model. Our calculated hole mobility at room temperature is 17.12 cm^2/(V s) for C$_{42}$H$_{28}$ and 16.68 cm^2/(V s) for C$_{42}$D$_{28}$, and the isotope effect on mobility is found to be as small as −2.57%. The results agree well with experiment that both C$_{42}$H$_{28}$ and C$_{42}$D$_{28}$ crystals exhibited room-temperature mobility of ~15 cm^2/(V s). The calculated results demonstrate that all-deuteration on rubrene (C$_{42}$D$_{28}$) has a slight isotope effect on charge transport. For comparison, the isotope effect of all-deuterated tetracene, the parent of rubrene, has been computed and found to be only −0.53%, which also shows no deuteration effect. For all-deuterated rubrene and tetracene, the situation is similar to **N3** and **P3** that replacing the aromatic H by D can cause little impact on vibrational modes with large reorganization energy. Therefore, for understanding the intrinsic transport properties in rubrene and tetracene, we can try to find other isotopic substitutions with a dramatic isotope effect theoretically in the future.

To summarize, we propose a feasible scheme to examine the transport mechanism in organic semiconductors based on the quantum nuclear tunneling model. We predict an isotope effect in the hopping transport process. For the band-like transport with acoustic phonon dominance, there is no isotope effect. SC Marcus theory has gained wide popularity for studying organic semiconductors, by which there is no isotope effect either. We emphasize here that the isotope substitution tends to reduce the carrier mobility due to the nuclear tunneling effect. We take typical n-type materials, alkyl-substituted NDI and PDI, as examples to first demonstrate how the isotope effect can occur. All-deuteration on side chains can reduce mobility by ~18% for NDI-C6 and by ~13% for PDI-C8. Moreover, all ^{13}C-substitution on the backbone can reduce the mobility by ~7 and 10% for NDI-C6 and PDI-C8 separately. In contrast, all-deuteration on the backbone of NDI-C6 or PDI-C8 has nearly no isotope effect on charge transport, and partial backbone ^{13}C-substituted NDI-C6 also shows much less isotope effect than all-backbone ^{13}C-substituted. For rubrene and tetracene, all-deuteration on the whole molecule still shows little isotope effect. Therefore, in the hopping systems, the necessary condition for noticeable isotope effect on transport is that the isotopic substitution position should be involved actively in the

Table 2. Frequencies (cm^{-1}) of the Five Vibrational Normal Modes Presented in Figure 3 for All Isotopic NDI-C6's^a

NDI-C6	mode frequency				
	1	2	3	4	5
N0	405.41	557.00	1450.90	1646.63	1781.34
N1	391.65	551.47	1446.22	1632.79	1779.00
	(3.39%)	(0.99%)	(0.32%)	(0.84%)	(0.13%)
N2	392.17	556.55	1450.37	1646.62	1779.16
	(3.26%)	(0.08%)	(0.04%)	(0.00%)	(0.12%)
N3	404.39	552.99	1446.24	1632.82	1781.18
	(0.25%)	(0.72%)	(0.32%)	(0.83%)	(0.01%)
N4	404.77	546.09	1394.99	1585.83	1735.63
	(0.16%)	(1.96%)	(3.85%)	(3.69%)	(2.57%)
N5	405.14	554.78	1424.78	1632.27	1780.51
	(0.07%)	(0.40%)	(1.80%)	(0.87%)	(0.05%)

^{a}The relative reductions of frequencies for five isotopic NDI-C6's compared to **N0** are labeled in parentheses.

relevant vibrations with appreciable contributions to the charge reorganization energy and electron−phonon coupling. By studying the isotope effect on mobility for such a kind of isotopic substitution, the transport mechanism in pristine systems may reveal whether there is a nuclear tunneling effect and whether the hopping or the band-like transport is dominant.

METHODOLOGY

The neutral and charged geometries of all isotopic substitutions are optimized with B3LYP/6-31G(d)[51,52] by the Gaussian 09 package,[53] and the equilibrium geometries of isotopic systems are completely the same. The total reorganization energies obtained from the adiabatic potential method are identical, which are 350 meV for all NDI-C6 systems, 271 meV for all PDI-C8 systems, and 150 meV for all rubrenes. Vibrational frequencies are calculated at the same level. With the help of the DUSHIN program,[54] the corresponding Huang−Rhys factors and reorganization energies are obtained via normal-mode analysis under the displaced harmonic oscillator approximation. The total reorganization energies obtained from normal-mode relaxation are 351, 272, and 151 meV for NDIs, PDIs, and rubrenes, respectively, essentially the same as the adiabatic potential model, indicating the applicability of the harmonic oscillator approximation.

We assume the same crystal structures[40,41,55] for different isotopes. According to the benchmark studies on the basis set and exchange−correlation functional for evaluating electronic coupling,[56] PW91PW91/6-31G(d)[57] is employed to calculate the intermolecular integral for all of the neighboring molecular pairs. The transfer integrals of different isotopic substitutions are exactly the same for different systems, with the largest values of 74, 44, and 83 meV for NDIs, PDIs, and rubrenes, respectively. Thus, NDI-C6 and PDI-C8 are typical hopping models for $\lambda \gg V$, while rubrene is close to the band-like model.

It is noted that the time integration of eq 1 is of oscillating behavior, which is only convergent when S is large. In fact, for rubrene, because the phenyl twisting motions possess a large Huang−Rhys factor, the numerical integration is convergent. However, for NDI and PDI, there is no such dominant mode to guarantee convergence. Thus, we add a Lorentzian $e^{-\Gamma|t|}$ factor with a very small broadening of $\Gamma = 10$ cm^{-1} for both NDI and PDI, which can be regarded as dissipation from the environments.

ASSOCIATED CONTENT

Ⓢ Supporting Information

The theoretical results of the isotope effect on the band-like mobility by Boltzmann theory and the deformation potential theory, full quantum CT rates and corresponding isotope effects for NDI-C6, PDI-C8, and rubrene systems, as well as normal-mode analysis are presented. This material is available free of charge via the Internet at http://pubs.acs.org.

AUTHOR INFORMATION

Corresponding Author

*E-mail: zgshuai@tsinghua.edu.cn.

Notes

The authors declare no competing financial interest.

REFERENCES

(1) Xie, W.; Willa, K.; Wu, Y.; Häusermann, R.; Takimiya, K.; Batlogg, B.; Frisbie, C. D. Temperature-Independent Transport in High-Mobility Dinaphtho-Thieno-Thiophene (DNTT) Single Crystal Transistors. *Adv. Mater.* **2013**, *25*, 3478−3484.

(2) Wang, M.; Li, J.; Zhao, G.; Wu, Q.; Huang, Y.; Hu, W.; Gao, X.; Li, H.; Zhu, D. High-Performance Organic Field-Effect Transistors Based on Single and Large-Area Aligned Crystalline Microribbons of 6,13-Dichloropentacene. *Adv. Mater.* **2013**, *25*, 2229−2233.

(3) He, T.; Stolte, M.; Würthner, F. Air-Stable N-Channel Organic Single Crystal Field-Effect Transistors Based on Microribbons of Core-Chlorinated Naphthalene Diimide. *Adv. Mater.* **2013**, *25*, 6951−6955.

(4) Brédas, J. L.; Calbert, J. P.; da Silva Filho, D. A.; Cornil, J. Organic Semiconductors: A Theoretical Characterization of the Basic Parameters Governing Charge Transport. *Proc. Natl. Acad. Sci. U.S.A.* **2002**, *99*, 5804−5809.

(5) Cornil, J.; Beljonne, D.; Calbert, J. P.; Brédas, J. L. Interchain Interactions in Organic Π-Conjugated Materials: Impact on Electronic Structure, Optical Response, and Charge Transport. *Adv. Mater.* **2001**, *13*, 1053−1067.

(6) Coropceanu, V.; Cornil, J.; da Silva Filho, D. A.; Olivier, Y.; Silbey, R.; Brédas, J.-L. Charge Transport in Organic Semiconductors. *Chem. Rev.* **2007**, *107*, 926−952.

(7) Song, Y.; Di, C. a.; Yang, X.; Li, S.; Xu, W.; Liu, Y.; Yang, L.; Shuai, Z.; Zhang, D.; Zhu, D. A Cyclic Triphenylamine Dimer for Organic Field-Effect Transistors with High Performance. *J. Am. Chem. Soc.* **2006**, *128*, 15940−15941.

(8) Sokolov, A. N.; Atahan-Evrenk, S.; Mondal, R.; Akkerman, H. B.; Sánchez-Carrera, R. S.; Granados-Focil, S.; Schrier, J.; Mannsfeld, S. C.; Zoombelt, A. P.; Bao, Z. From Computational Discovery to Experimental Characterization of a High Hole Mobility Organic Crystal. *Nat. Commun.* **2011**, *2*, 437−444.

(9) Chang, Y.-C.; Chao, I. An Important Key to Design Molecules with Small Internal Reorganization Energy: Strong Nonbonding Character in Frontier Orbitals. *J. Phys. Chem. Lett.* **2009**, *1*, 116−121.

(10) Fratini, S.; Ciuchi, S. Bandlike Motion and Mobility Saturation in Organic Molecular Semiconductors. *Phys. Rev. Lett.* **2009**, *103*, 266601/1−266601/4.

(11) Podzorov, V.; Menard, E.; Borissov, A.; Kiryukhin, V.; Rogers, J. A.; Gershenson, M. E. Intrinsic Charge Transport on the Surface of Organic Semiconductors. *Phys. Rev. Lett.* **2004**, *93*, 086602/1−086602/4.

(12) Troisi, A.; Orlandi, G. Charge-Transport Regime of Crystalline Organic Semiconductors: Diffusion Limited by Thermal Off-Diagonal Electronic Disorder. *Phys. Rev. Lett.* **2006**, *96*, 086601/1−086601/4.

(13) Troisi, A. Charge Transport in High Mobility Molecular Semiconductors: Classical Models and New Theories. *Chem. Soc. Rev.* **2011**, *40*, 2347−2358.

(14) Chang, J.-F.; Sakanoue, T.; Olivier, Y.; Uemura, T.; Dufourg-Madec, M.-B.; Yeates, S. G.; Cornil, J.; Takeya, J.; Troisi, A.; Sirringhaus, H. Hall-Effect Measurements Probing the Degree of Charge-Carrier Delocalization in Solution-Processed Crystalline Molecular Semiconductors. *Phys. Rev. Lett.* **2011**, *107*, 066601/1−066601/4.

(15) Sakanoue, T.; Sirringhaus, H. Band-Like Temperature Dependence of Mobility in a Solution-Processed Organic Semiconductor. *Nat. Mater.* **2010**, *9*, 736−740.

(16) Nan, G.; Yang, X.; Wang, L.; Shuai, Z.; Zhao, Y. Nuclear Tunneling Effects of Charge Transport in Rubrene, Tetracene, and Pentacene. *Phys. Rev. B* **2009**, *79*, 115203/1−115203/9.

(17) Geng, H.; Peng, Q.; Wang, L.; Li, H.; Liao, Y.; Ma, Z.; Shuai, Z. Toward Quantitative Prediction of Charge Mobility in Organic Semiconductors: Tunneling Enabled Hopping Model. *Adv. Mater.* **2012**, *24*, 3568−3572.

(18) Lin, S. H.; Chang, C. H.; Liang, K. K.; Chang, R.; Shiu, Y. J.; Zhang, J. M.; Yang, T. S.; Hayashi, M.; Hsu, F. C. Ultrafast Dynamics and Spectroscopy of Bacterial Photosynthetic Reaction Centers. *Adv. Chem. Phys.* **2002**, *121*, 1−88.

(19) Yuen, J. D.; Menon, R.; Coates, N. E.; Namdas, E. B.; Cho, S.; Hannahs, S. T.; Moses, D.; Heeger, A. J. Nonlinear Transport in Semiconducting Polymers at High Carrier Densities. *Nat. Mater.* **2009**, *8*, 572−575.

(20) Kronemeijer, A. J.; Huisman, E. H.; Katsouras, I.; van Hal, P. A.; Geuns, T. C. T.; Blom, P. W. M.; van der Molen, S. J.; de Leeuw, D. M. Universal Scaling in Highly Doped Conducting Polymer Films. *Phys. Rev. Lett.* **2010**, *105*, 156604/1−156604/4.

(21) Rodin, A. S.; Fogler, M. M. Apparent Power-Law Behavior of Conductance in Disordered Quasi-One-Dimensional Systems. *Phys. Rev. Lett.* **2010**, *105*, 106801/1−106801/4.

(22) Asadi, K.; Kronemeijer, A. J.; Cramer, T.; Jan Anton Koster, L.; Blom, P. W. M.; de Leeuw, D. M. Polaron Hopping Mediated by Nuclear Tunnelling in Semiconducting Polymers at High Carrier Density. *Nat. Commun.* **2013**, *4*, 1710−1718.

(23) Morteani, A. C.; Dhoot, A. S.; Kim, J. S.; Silva, C.; Greenham, N. C.; Murphy, C.; Moons, E.; Ciná, S.; Burroughes, J. H.; Friend, R. H. Barrier-Free Electron−Hole Capture in Polymer Blend Hetero-junction Light-Emitting Diodes. *Adv. Mater.* **2003**, *15*, 1708−1712.

(24) Panzer, M. J.; Frisbie, C. D. High Carrier Density and Metallic Conductivity in Poly(3-hexylthiophene) Achieved by Electrostatic Charge Injection. *Adv. Funct. Mater.* **2006**, *16*, 1051−1056.

(25) Zhong, X.; Zhao, Y. Charge Carrier Dynamics in Phonon-Induced Fluctuation Systems from Time-Dependent Wavepacket Diffusion Approach. *J. Chem. Phys.* **2011**, *135*, 134110/1−134110/10.

(26) Zhong, X.; Zhao, Y. Non-Markovian Stochastic Schrödinger Equation at Finite Temperatures for Charge Carrier Dynamics in Organic Crystals. *J. Chem. Phys.* **2013**, *138*, 014111/1−014111/9.

(27) Zhang, W.; Zhong, X.; Zhao, Y. Electron Mobilities of N-Type Organic Semiconductors from Time-Dependent Wavepacket Diffusion Method: Pentacenequinone Derivatives. *J. Phys. Chem. A* **2012**, *116*, 11075−11082.

(28) Gorham-Bergeron, E.; Emin, D. Phonon-Assisted Hopping Due to Interaction with Both Acoustical and Optical Phonons. *Phys. Rev. B* **1977**, *15*, 3667−3680.

(29) Ulstrup, J.; Jortner, J. The Effect of Intramolecular Quantum Modes on Free Energy Relationships for Electron Transfer Reactions. *J. Chem. Phys.* **1975**, *63*, 4358−4368.

(30) Tang, L.; Long, M.; Wang, D.; Shuai, Z. The Role of Acoustic Phonon Scattering in Charge Transport in Organic Semiconductors: A First-Principles Deformation-Potential Study. *Sci. China Ser. B: Chem.* **2009**, *52*, 1646−1652.

(31) Shi, W.; Chen, J.; Xi, J.; Wang, D.; Shuai, Z. Search for Organic Thermoelectric Materials with High Mobility: The Case of 2,7-Dialkyl[1]Benzothieno[3,2-B][1]Benzothiophene Derivatives. *Chem. Mater.* **2014**, *26*, 2669−2677.

(32) Xie, W.; McGarry, K. A.; Liu, F.; Wu, Y.; Ruden, P. P.; Douglas, C. J.; Frisbie, C. D. High-Mobility Transistors Based on Single Crystals of Isotopically Substituted Rubrene-D28. *J. Phys. Chem. C* **2013**, *117*, 11522−11529.

(33) Bigeleisen, J.; Wolfsberg, M. Theoretical and Experimental Aspects of Isotope Effects in Chemical Kinetics. *Adv. Chem. Phys.* **1958**, *1*, 15−76.

(34) Ludlow, M. K.; Soudackov, A. V.; Hammes-Schiffer, S. Theoretical Analysis of the Unusual Temperature Dependence of the Kinetic Isotope Effect in Quinol Oxidation. *J. Am. Chem. Soc.* **2009**, *131*, 7094−7102.

(35) Hazra, A.; Soudackov, A. V.; Hammes-Schiffer, S. Isotope Effects on the Nonequilibrium Dynamics of Ultrafast Photoinduced Proton-Coupled Electron Transfer Reactions in Solution. *J. Phys. Chem. Lett.* **2010**, *2*, 36−40.

(36) Lin, S. H.; Bersohn, R. Effect of Partial Deuteration and Temperature on Triplet-State Lifetimes. *J. Chem. Phys.* **1968**, *48*, 2732−2736.

(37) Saltiel, J.; Waller, A. S.; Sears, D. F.; Garrett, C. Z. Fluorescence Quantum Yields of *trans*-Stilbene-d_0 and *trans*-Stilbene-d_2 in *n*-Hexane and *n*-Tetradecane. Medium and Deuterium Isotope Effects on Decay Processes. *J. Phys. Chem.* **1993**, *97*, 2516−2522.

(38) Hewitt, J. T.; Concepcion, J. J.; Damrauer, N. H. Inverse Kinetic Isotope Effect in the Excited-State Relaxation of a Ru(II)−Aquo Complex: Revealing the Impact of Hydrogen-Bond Dynamics on Nonradiative Decay. *J. Am. Chem. Soc.* **2013**, *135*, 12500−12503.

(39) Zhan, X. W.; Facchetti, A.; Barlow, S.; Marks, T. J.; Ratner, M. A.; Wasielewski, M. R.; Marder, S. R. Rylene and Related Diimides for Organic Electronics. *Adv. Mater.* **2011**, *23*, 268−284.

(40) Shukla, D.; Nelson, S. F.; Freeman, D. C.; Rajeswaran, M.; Ahearn, W. G.; Meyer, D. M.; Carey, J. T. Thin-Film Morphology Control in Naphthalene-Diimide-Based Semiconductors: High Mobility N-Type Semiconductor for Organic Thin-Film Transistors. *Chem. Mater.* **2008**, *20*, 7486−7491.

(41) Briseno, A. L.; Mannsfeld, S. C. B.; Reese, C.; Hancock, J. M.; Xiong, Y.; Jenekhe, S. A.; Bao, Z.; Xia, Y. Perylenediimide Nanowires and Their Use in Fabricating Field-Effect Transistors and Comple-mentary Inverters. *Nano Lett.* **2007**, *7*, 2847−2853.

(42) Chesterfield, R. J.; McKeen, J. C.; Newman, C. R.; Ewbank, P. C.; da Silva Filho, D. A.; Brédas, J.-L.; Miller, L. L.; Mann, K. R.; Frisbie, C. D. Organic Thin Film Transistors Based on N-Alkyl Perylene Diimides: Charge Transport Kinetics as a Function of Gate Voltage and Temperature. *J. Phys. Chem. B* **2004**, *108*, 19281−19292.

(43) Li, X.-Y. Electron Transfer between Tryptophan and Tyrosine: Theoretical Calculation of Electron Transfer Matrix Element for Intramolecular Hole Transfer. *J. Comput. Chem.* **2001**, *22*, 565−579.

(44) Troisi, A.; Orlandi, G. The Hole Transfer in DNA: Calculation of Electron Coupling between Close Bases. *Chem. Phys. Lett.* **2001**, *344*, 509−518.

(45) Fujita, T.; Nakai, H.; Nakatsuji, H. Ab Initio Molecular Orbital Model of Scanning Tunneling Microscopy. *J. Chem. Phys.* **1996**, *104*, 2410−2417.

(46) Valeev, E. F.; Coropceanu, V.; da Silva Filho, D. A.; Salman, S.; Brédas, J.-L. Effect of Electronic Polarization on Charge-Transport Parameters in Molecular Organic Semiconductors. *J. Am. Chem. Soc.* **2006**, *128*, 9882−9886.

(47) Nan, G.; Wang, L.; Yang, X.; Shuai, Z.; Zhao, Y. Charge Transfer Rates in Organic Semiconductors Beyond First-Order Perturbation: From Weak to Strong Coupling Regimes. *J. Chem. Phys.* **2009**, *130*, 024704/1−024704/8.

(48) Young, W. M.; Elcock, E. W. Monte Carlo Studies of Vacancy Migration in Binary Ordered Alloys: I. *Proc. Phys. Soc.* **1966**, *89*, 735.

(49) Minder, N. A.; Ono, S.; Chen, Z.; Facchetti, A.; Morpurgo, A. F. Band-Like Electron Transport in Organic Transistors and Implication of the Molecular Structure for Performance Optimization. *Adv. Mater.* **2012**, *24*, 503−508.

(50) Lee, B.; Chen, Y.; Fu, D.; Yi, H.; Czelen, K.; Najafov, H.; Podzorov, V. Trap Healing and Ultralow-Noise Hall Effect at the Surface of Organic Semiconductors. *Nat. Mater.* **2013**, *12*, 1125−1129.

(51) Becke, A. D. Density-Functional Thermochemistry. III. The Role of Exact Exchange. *J. Chem. Phys.* **1993**, *98*, 5648−5652.

(52) Lee, C.; Yang, W.; Parr, R. G. Development of the Colle−Salvetti Correlation-Energy Formula into a Functional of the Electron Density. *Phys. Rev. B* **1988**, *37*, 785−789.

(53) Frisch, M. J.; Trucks, G. W.; Schlegel, H. B.; Scuseria, G. E.; Robb, M. A.; Cheeseman, J. R.; Scalmani, G.; Barone, V.; Mennucci, B.; Petersson, G. A.; et al. *Gaussian 09*, revision A.02; Gaussian, Inc.: Wallingford, CT, 2009.

(54) Reimers, J. R. A Practical Method for the Use of Curvilinear Coordinates in Calculations of Normal-Mode-Projected Displace-ments and Duschinsky Rotation Matrices for Large Molecules. *J. Chem. Phys.* **2001**, *115*, 9103−9109.

(55) Jurchescu, O. D.; Meetsma, A.; Palstra, T. T. Low-Temperature Structure of Rubrene Single Crystals Grown by Vapor Transport. *Acta Crystallogr., Sect. B* **2006**, *62*, 330−334.

(56) Nan, G.; Li, Z. Influence of Lattice Dynamics on Charge Transport in the Dianthra [2,3-B:2′,3′-F]-Thieno [3,2-B] Thiophene Organic Crystals from a Theoretical Study. *Phys. Chem. Chem. Phys.* **2012**, *14*, 9451−9459.

(57) Perdew, J. P.; Chevary, J. A.; Vosko, S. H.; Jackson, K. A.; Pederson, M. R.; Singh, D. J.; Fiolhais, C. Atoms, Molecules, Solids, and Surfaces: Applications of the Generalized Gradient Approximation for Exchange and Correlation. *Phys. Rev. B* **1992**, *46*, 6671−6687.

2273

dx.doi.org/10.1021/jz500825q | *J. Phys. Chem. Lett.* 2014, 5, 2267−2273